ChemComm

Transcription-induced formation of paired Al sites in high-silica CHA-type zeolite framework using Al-rich amorphous aluminosilicate

Journal:	*ChemComm*
Manuscript ID	CC-COM-09-2021-005401.R1
Article Type:	Communication

COMMUNICATION

Transcription-induced formation of paired Al sites in high-silica CHA-type zeolite framework using Al-rich amorphous aluminosilicate†

Received 00th January 20xx,
Accepted 00th January 20xx

DOI: 10.1039/x0xx00000x

Mizuho Yabushita,*[,a] Yoshiyasu Imanishi,[§,b] Ting Xiao,[§,b,c] Ryota Osuga,[b] Toshiki Nishitoba,[§§,d] Sachiko Maki,[b,e] Kiyoshi Kanie,[b,e] Wenbin Cao,[c] Toshiyuki Yokoi[d] and Atsushi Muramatsu*[,b,e,f]

The paired Al species pre-formed in Al-rich amorphous aluminosilicates were transcribed into high-silica CHA-type zeolite frameworks under hydrothermal conditions, which offers a new approach to creating paired Al sites in zeolite frameworks. This Al-pair-rich CHA exhibited a higher Sr^{2+} uptake than the control CHA zeolite synthesized by the conventional procedure.

Fine-tuning of the structure of zeolites, which are crystalline, porous aluminosilicates and have been a key component of the chemical industry for decades,[1–6] is a promising approach to the development of superior functional materials. The isomorphous substitution of Al^{3+} into a tetrahedral site (T-site) of the zeolite framework provides one negative charge in a one-to-one manner, which functions as an ion-exchange site for a monovalent cation. The capture of divalent cations by a zeolite surface via ion exchange is beneficial in water purification[7,8] and the production of unique catalysts, where deposited divalent metal cations serve as active sites.[9,10] For such objectives, given the widely accepted Loewenstein's rule, according to which nearest neighboring Al pairs (*i.e.*, the Al–O–Al sequence) cannot form because of their poor stability,[11] the zeolite frameworks need to be enriched by ion-exchange sites consisting of second and third nearest neighboring Al pairs referred to as Al–O–(Si–O)$_x$–Al (x = 1 or 2) sequences. A simple approach to increasing the Al content in frameworks enhances the probability for the formation of such juxtaposed sites but cannot be applied to high-silica zeolites with Si/Al ratios of ≥ 5. Thus, a reliable synthesis strategy capable of pairing Al^{3+} species in zeolite frameworks—where ideally, all Al atoms occupy pair sites—needs to be devised.[12–14]

For a **CHA**-type framework, which possesses single crystallographically distinct T-sites,[15] several approaches have been devised thus far. Gounder *et al.* reported that the combination of two structure-directing agents (SDAs) comprising the small Na^+ ion and the bulky *N*,*N*,*N*-trimethyl-1-adamantylammonium cation ($TMAda^+$), the latter of which is a typical SDA used for synthesizing **CHA** zeolites,[5,16] led to the formation of Al pair sites even in the high-silica region (*i.e.*, Si/Al = 15–30) because of electrostatic interactions between these positively charged SDAs and negatively charged Al-containing complexes that are formed from substances (*i.e.*, SiO_2 and $Al(OH)_3$) during hydrothermal processes (Fig. 1).[17,18] The fraction of Al^{3+} involved in pair sites increased linearly with increasing Na^+ loading in the synthesis gels. The thus-formed Al pair sites provided a higher rate constant for propane cracking than isolated Al sites.[19] In terms of a more complicated framework **MFI**, where twelve crystallographically different T-sites are present,[15] Dědeček *et al.* demonstrated that the sources of Si and Al impacted the content of Al pair sites.[20] For these synthesis systems, which rely on homogeneous substances including SDA(s) and sources of Si and Al, van der Waals and electrostatic interactions induced between those compounds are responsible for the content of Al pair sites in the resulting zeolite specimens.[21] Alternatively, Yokoi *et al.* found that the interzeolite conversion of an **FAU** zeolite enriched with paired Al sites owing to its high Al content (Si/Al = 2.4–2.8) provided a **CHA** zeolite with a large fraction of Al in pair sites (Fig. 1).[22,23] In our related work, amorphous metallosilicates were transformed hydrothermally into a variety of metal-substituted zeolite frameworks.[24–29] These reports using solid

[a.] *Department of Applied Chemistry, School of Engineering, Tohoku University, 6-6-07 Aoba, Aramaki, Aoba-ku, Sendai, Miyagi 980-8579, Japan. E-mail: m.yabushita@tohoku.ac.jp*
[b.] *Institute of Multidisciplinary Research for Advanced Materials, Tohoku University, 2-1-1 Katahira, Aoba-ku, Sendai, Miyagi 980-8577, Japan. E-mail: mura@tohoku.ac.jp*
[c.] *Department of Inorganic Nonmetallic Materials, School of Materials Science and Engineering, University of Science and Technology Beijing, Beijing 100083, China*
[d.] *Institute of Innovative Research, Tokyo Institute of Technology, 4259 Nagatsuta-cho, Midori-ku, Yokohama, Kanagawa 226-8503, Japan*
[e.] *International Center for Synchrotron Radiation Innovation Smart, Tohoku University, 2-1-1 Katahira, Aoba-ku, Sendai, Miyagi 980-8577, Japan*
[f.] *Core Research for Evolutional Science and Technology, Japan Science and Technology Agency, 4-1-8 Honcho, Kawaguchi, Saitama 332-0012, Japan*

† Electronic Supplementary Information (ESI) available: Experimental and characterization data for Al-rich amorphous aluminosilicate, CHA-t_2, and SSZ-13. See DOI: 10.1039/x0xx00000x

§ These authors contributed equally to this work.

§§ Current address: National Institute of Advanced Industrial Science and Technology, 1-1-1 Higashi, Tsukuba Central 5, Tsukuba, Ibaraki 305-8565, Japan

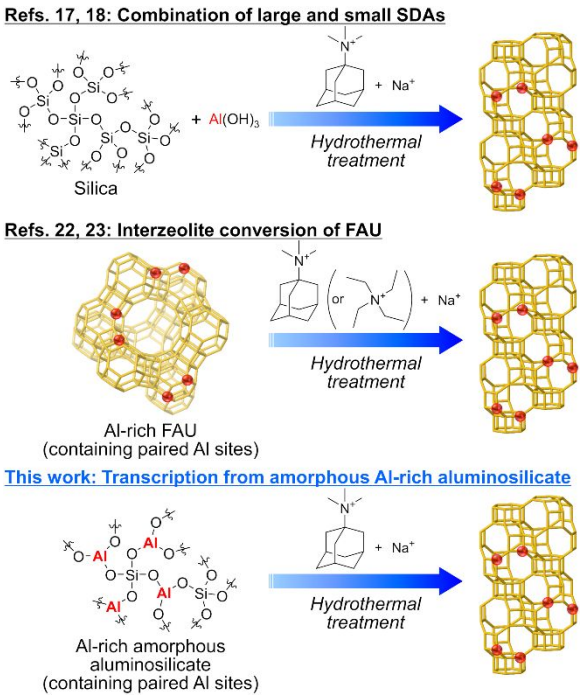

Fig. 1 Reported and current approaches to the formation of paired Al sites in **CHA**-type zeolite framework.

metallosilicates as precursors suggest that building blocks dissolve from such precursors and subsequently precipitate as zeolites; in other words, the local structure pre-formed in metallosilicate precursors such as Si–O–M units (M: substituting metal) are transcribed into the resulting zeolite frameworks. These previous reports and mechanistic insights inspired us to employ an Al-rich aluminosilicate containing a large quantity of Al–O–Si–O–Al sequences as a precursor to Al-pair-rich zeolites (Fig. 1), which is a novel approach to creating paired Al sites.

Based on this synthesis strategy, first, an aluminosilicate with a Si/Al ratio of 2.5 was prepared via a kind of sol-gel method known as the polymerized complex method,[30] where propylene-glycol modified silane[31] and $Al(NO_3)_3$ were used as starting reagents (see Experimental and Fig. S1, ESI†), as reported in our previous paper.[29] Powder X-ray diffraction (XRD) measurements and ^{29}Si magic angle spinning nuclear magnetic resonance (^{29}Si MAS NMR) spectroscopy revealed the presence of various Si species, $Si(OSi)_{4-n}(OAl)_n$ ($0 \le n \le 4$) referred to as $Q^4(nAl)$,[32] including the desired $Q^4(2Al)$ units (*i.e.*, Al–O–Si–O–Al sequence) in the thus-prepared amorphous aluminosilicate, and the cross polarization (CP) technique showed the absence of $Si(OT)_{4-y}(OH)_y$ (T = Si or Al, $1 \le y \le 3$) species (see Fig. S2 and Table S1, ESI†). Given the formation of such desired species, this specimen was employed in the subsequent step.

The second step was a hydrothermal process for synthesizing **CHA**-type zeolites. **CHA**-type zeolites were targeted in this work for the ease in understanding their structure due to the presence of single T-sites.[15] Prior to the hydrothermal treatment at 443 K for 5 days, the aging process at room temperature for the synthesis gels was examined. Under basic conditions, the amorphous aluminosilicate containing the pre-formed desirable building blocks undergoes hydrolysis to be dissolved in a liquid phase, indicating that the degree of hydrolysis needs to be carefully controlled. The detailed procedure is described in the Experimental section and Fig. S1 (ESI†). Briefly, the provisional synthesis gels were prepared by mixing SiO_2 (for controlling the Si/Al ratio of the gels), SDAs (TMAdaOH and NaOH), and deionized water and stirred at room temperature for t_1 hours. After the addition of the amorphous aluminosilicate into the gels as a source of both Si and Al, the resulting gels with a Si/Al ratio of 10 based on the loading amounts of starting reagents were further aged at room temperature for t_2 hours. In all cases, the total aging time (*i.e.*, $t_1 + t_2$) was kept constant at 48 h; in other words, the degree of hydrolysis of the amorphous aluminosilicate was altered by varying the duration of its exposure to basic solutions. Fig. 2 shows XRD patterns for solid samples that were hydrothermally synthesized by varying the aging parameter t_2 from 0 to 48 h. The consistency between each pattern and the reference demonstrated the successful construction of a **CHA**-type framework in the hydrothermal process, regardless of t_2. Hereafter, the hydrothermally synthesized **CHA** zeolite samples will be denoted as CHA-t_2. Inductively coupled plasma-atomic emission spectroscopy (ICP-AES) revealed that, regardless of the value of t_2, the Si/Al ratios of the CHA-t_2 samples fell in the narrow range between 5.7 and 5.8 (Table 1). Therefore, all CHA-t_2 samples were categorized as high-silica zeolites. These Si/Al ratios were lower than the value calculated from the amounts of reagents used (*i.e.*, 10), indicating that a part of the Si species derived from the additional SiO_2 remained dissolved in a liquid phase, similarly to our previous studies in which zeotype materials were synthesized hydrothermally from amorphous metallosilicates;[29,33] indeed, the yields of solid CHA-t_2 samples were in the 50–57% range (Table 1). The specific surface area for each CHA-t_2 calculated from the N_2 physisorption data (Fig. S3, ESI†) and the Brunauer-Emmett-Teller (BET) equation was *ca.* 700 $m^2\ g^{-1}$. The consistency of these textural properties for all the synthesized CHA-t_2 samples allowed us to directly compare the proportion of paired Al species.

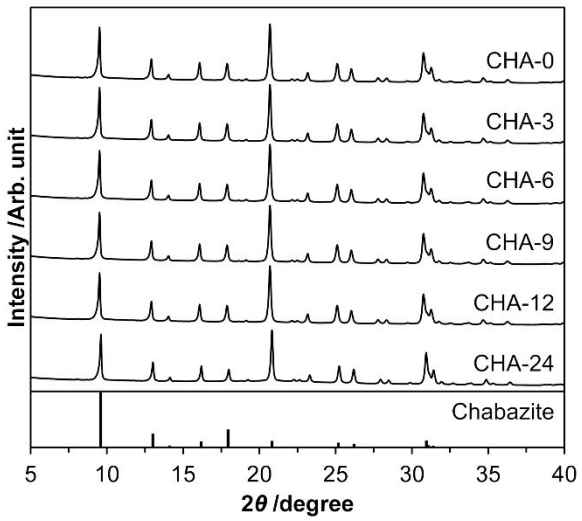

Fig. 2 Framework structure of CHA-t_2 synthesized from Al-rich amorphous aluminosilicate, characterized by XRD. Reference: chabazite (**CHA** zeolite, ICSD card #84255).

Table 1 Textural properties of CHA-t_2 samples.

Sample	Yield[a] /%	Si/Al[b]	S_{BET}[c] /m^2 g^{-1}	V_{total}[d] /cm^3 g^{-1}	Proportion of Q^4(nAl)[e] /%			Proportion of Al-containing Q^4(nAl)[f] /%		Sr uptake[g] /mg $g_{zeolite}^{-1}$
					Q^4(0Al)	Q^4(1Al)	Q^4(2Al)	Q^4(1Al)	Q^4(2Al)	
CHA-0	52	5.7	700	0.27	49	44	6.9	86	14	9.7 ± 0.2
CHA-3	55	5.8	690	0.26	49	43	7.5	85	15	13 ± 1.2
CHA-6	52	5.7	700	0.26	47	43	10	81	19	31 ± 5.0
CHA-9	57	5.7	700	0.26	46	42	12	77	23	50 ± 1.6
CHA-12	50	5.8	700	0.26	48	44	7.6	85	15	32 ± 4.2
CHA-24	50	5.8	700	0.26	50	43	7.4	85	15	32 ± 4.5

[a] Yield of the solid product, calculated by dividing the mass of each calcined CHA-t_2 sample by the total mass of the dried solid reagents (*i.e.*, amorphous aluminosilicate, additional SiO_2, and seed crystal). [b] Determined via ICP-AES after complete sample dissolution in aqueous HF solution. [c] BET specific surface area, estimated from the N_2 adsorption data (Fig. S3, ESI†) in the appropriate p/p_0 range where the *C* value in the BET equation to be positive. [d] Total pore volume, evaluated from the N_2 physisorpiton data at p/p_0 = 0.95 (Fig. S3, ESI†). [e] Estimated from the areas of each Q^4(nAl) peak in ^{29}Si MAS NMR spectra (see Figs. S4 and S5, ESI†): (Proportion of Q^4(nAl) (n = 0–2)) = (Peak area for Q^4(nAl)) / ((Peak area for Q^4(0Al)) + (Peak area for Q^4(1Al)) + (Peak area for Q^4(2Al))). [f] (Proportion of Al-containing Q^4(nAl) (n = 1 or 2)) = (Peak area for Q^4(nAl)) / ((Peak area for Q^4(1Al)) + (Peak area for Q^4(2Al))). [g]Sr uptake measured after ion exchange in an aqueous $SrCl_2$ solution.

A series of CHA-t_2 specimens was characterized using ^{27}Al and ^{29}Si MAS NMR spectroscopy to investigate the coordinating structure of both atoms in these samples. In the ^{27}Al MAS NMR spectra in Fig. S4A (ESI†), a peak at 57–58 ppm, assignable to tetrahedrally coordinated Al species incorporated into the zeolite framework,[32] was observed, with no other peaks, indicating that all Al atoms were successfully taken in the **CHA** framework without the formation of extra-framework Al species. The ^{29}Si MAS NMR spectra in Fig. S4B (ESI†) demonstrated the presence of three different Si species, *viz.*, Q^4(0Al) at –111 ppm, Q^4(1Al) at –105 ppm, and Q^4(2Al) at –98.5 ppm,[32] in each CHA-t_2 sample. Note that these peaks did not overlap with any other peaks attributable to $Si(OT)_{4-y}(OH)_y$ (T = Si or Al, $1 \le y \le 3$) species because no peak was observed in the ^{29}Si CP/MAS NMR spectra in Fig. S4C (ESI†). Table 1 summarizes the proportion of Q^4(nAl) species determined from the ^{29}Si MAS NMR spectra (Fig. S5, ESI†). The proportion of Q^4(2Al) to the total Al-containing Q^4(nAl) species increased from 14 to 23% upon an increase in t_2 from 0 to 9 h and decreased to 15% upon a further t_2 increase to 24 h. This volcano-type dependence of the Al proportion can be explained by our expectation already alluded to above: in the shorter aging time (*i.e.*, t_2 < 9 h), the hydrolysis and dissolution of the amorphous aluminosilicate caused by base (in this study, TMAdaOH and NaOH) were insufficient to supply proper building blocks containing Al–O–Si–O–Al sequence well, while the longer aging process (*i.e.*, t_2 > 9 h) rather led to further hydrolysis of such building blocks to lose the pre-formed sequence. The optimal aging time (t_2 = 9 h), therefore, led to the highest content of paired Al sites in the resulting **CHA**-type framework. This explanation is also supported by another volcano-type relationship between the aging time (t_2) and solid yield (Table 1). In addition to this transcription of the pre-formed structure of the amorphous aluminosilicate into the resulting zeolite framework, as demonstrated by Gounder *et al.*,[17,18] the combination of two SDAs, *i.e.*, the large $TMAda^+$ and small Na^+, allows both SDA molecules to be located simultaneously in the same cage of **CHA** framework and possibly also contributes to the formation of paired Al sites in our synthetic systems (see Fig. 1). In previous reports, the proportion of Q^4(2Al) to the total Al-containing Q^4(nAl) species for high-silica **CHA**-type zeolites examined by ^{29}Si MAS NMR spectroscopy was in the range between 18–30% (Table S2, ESI†),[22,23,34] which are comparable or even higher, compared to the highest Q^4(2Al) proportion achieved in this study (*i.e.*, 23%, Table 1). However, these reported procedures could not vary the proportion of Q^4(2Al) at the constant Si/Al ratio; in stark contrast, the data in Table 1 have demonstrated that the simple alteration of the aging time (t_2) for the amorphous aluminosilicate enables to control the Q^4(2Al) proportion at the same Si/Al level, which provides a unique opportunity to fairly investigate performance and role of isolated and paired Al sites in a variety of zeolite applications.

Considering the attractive function of paired Al sites in zeolites as ion-exchange sites that can capture divalent cations, the adsorption performance of CHA-t_2 samples for Sr^{2+}, one of whose isotopes, ^{90}Sr, is a radioactive pollutant found in radioactive waste liquids,[35–37] was elucidated. The uptake of Sr^{2+} increased from 9.7 ± 0.17 mg $g_{zeolite}^{-1}$ to 50 ± 1.6 mg $g_{zeolite}^{-1}$ upon an increase of the t_2 value from 0 to 9 h and decreased to 32 ± 4.5 mg $g_{zeolite}^{-1}$ with a further t_2 increase to 24 h (see Table 1). This trend roughly correlates with the proportion of Q^4(2Al) species and thus suggests that the paired Al sites behaved as ion exchange sites for Sr^{2+} ions. Although the proportion of Q^4(2Al) for CHA-3, CHA-12, and CHA-24 was the same, the latter two samples exhibited higher Sr^{2+} uptake. This contradiction could be due to the location of ion exchange sites on the paired Al sites; in CHA-3, each ion exchange site on the paired Al sites could face in different *cha*-cages and function as a monovalent ion exchange site. The control material SSZ-13, which is a typical **CHA**-type zeolite with uncontrolled Al species (see Experimental and Fig. S6, ESI†), showed the lower Sr^{2+} uptake (14 ± 0.3 mg $g_{zeolite}^{-1}$), compared to the CHA-t_2 samples except for CHA-0 and CHA-3. Even taking into consideration the difference of the Al contents, the Sr/Al molar ratio for the best ion exchanger CHA-

9 (Si/Al = 5.7) was 0.30, which was 2.7-fold higher than that for SSZ-13 (Si/Al = 7.1, Sr/Al = 0.11). This difference indicated the importance of the nature of ion-exchange sites; that is, the paired Al sites were effective in capturing divalent Sr^{2+} ions.

In conclusion, using amorphous aluminosilicate enriched by $Q^4(nAl)$ ($n \geq 2$) as a substrate, the hydrothermal process has successfully yielded **CHA**-type zeolites containing paired Al sites. The proportion of $Q^4(2Al)$ to the total Al-containing $Q^4(nAl)$ species can be varied in the range of 15–23% by simply altering the time of exposure of the amorphous aluminosilicate to the basic synthesis gels, since the degree of hydrolysis of the pre-formed building units is presumably important for the formation of paired Al sites in the resulting zeolite specimens. The thus-prepared **CHA** zeolites have also been demonstrated to exhibit better adsorption performance for the divalent cation Sr^{2+}, compared to the control ion exchanger SSZ-13. The novel approach to creating paired Al sites in zeolites using Al-rich aluminosilicate precursors reported here will open the door to the synthesis of unique zeolites and zeotype materials containing such juxtaposed heteroatom sites.

This work was supported financially by Core Research for Evolutional Science and Technology of the Japan Science and Technology Agency (Grant No. JPMJCR16P3), a Grant-in-Aid for Scientific Research (S) (21H05011) and a Grant-in-Aid for Early-Career Scientists (19K15355 and 21K14459) from the Japan Society for the Promotion of Science, the Kurita Water and Environment Foundation (21A023), the Nippon Life Insurance Foundation, and the Ministry of Education, Culture, Sports, Science, and Technology Dynamic Alliance for Open Innovation Bridging Human, Environment and Materials in Network Joint Research Center for Materials and Devices. T.X. is grateful for the scholarship granted to a visiting Ph.D. student of the Inter-University Exchange Project by China Scholarship Council (Scholarship No. 201906460114).

Conflicts of interest

There are no conflicts to declare.

References

1 T. F. Degnan Jr., *Top. Catal.*, 2000, **13**, 349–356.
2 J. Čejka, A. Corma and S. Zones, *Zeolites and catalysis: synthesis, reactions and applications*, Wiley-VCH, Weinheim, 2010.
3 Y. Li, L. Li and J. Yu, *Chem*, 2017, **3**, 928–949.
4 J. Přech, P. Pizarro, D. P. Serrano and J. Čejka, *Chem. Soc. Rev.*, 2018, **47**, 8263–8306.
5 M. Dusselier and M. E. Davis, *Chem. Rev.*, 2018, **118**, 5265–5329.
6 A. Deneyer, Q. Ke, J. Devos and M. Dusselier, *Chem. Mater.*, 2020, **32**, 4884–4919.
7 M. Jovanovic, N. Rajic and B. Obradovic, *J. Hazard. Mater.*, 2012, **233–234**, 57–64.
8 J. Perić, M. Trgo and N. V. Medvidović, *Water Res.*, 2004, **38**, 1893–1899.
9 J. Shan, W. Huang, L. Nguyen, Y. Yu, S. Zhang, Y. Li, A. I. Frenkel and F. Tao, *Langmuir*, 2014, **30**, 8558–8569.
10 B. Ipek, M. J. Wulfers, H. Kim, F. Göltl, I. Hermans, J. P. Smith, K. S. Booksh, C. M. Brown and R. F. Lobo, *ACS Catal.*, 2017, **7**, 4291–4303.
11 W. Loewenstein, *Am. Mineral.*, 1954, **39**, 92–96.
12 J. Dědeček, Z. Sobalík and B. Wichterlová, *Catal. Rev.*, 2012, **54**, 135–223.
13 J. Dědeček, E. Tabor and S. Sklenak, *ChemSusChem*, 2019, **12**, 556–576.
14 M. Yabushita, R. Osuga and A. Muramatsu, *CrystEngComm*, 2021, **23**, 6226–6233.
15 C. Baerlocher and L. B. McCusker, Database of Zeolite Structures, http://www.iza-structure.org/databases/, (accessed September 2021).
16 M. E. Davis and R. F. Lobo, *Chem. Mater.*, 1992, **4**, 756–768.
17 J. R. Di Iorio and R. Gounder, *Chem. Mater.*, 2016, **28**, 2236–2247.
18 J. R. Di Iorio, S. Li, C. B. Jones, C. T. Nimlos, Y. Wang, E. Kunkes, V. Vattipalli, S. Prasad, A. Moini, W. F. Schneider and R. Gounder, *J. Am. Chem. Soc.*, 2020, **142**, 4807–4819.
19 P. M. Kester, J. T. Crum, S. Li, W. F. Schneider and R. Gounder, *J. Catal.*, 2021, **395**, 210–226.
20 V. Gábová, J. Dědeček and J. Čejka, *Chem. Commun.*, 2003, 1196–1197.
21 J. Dedecek, V. Balgová, V. Pashkova, P. Klein and B. Wichterlová, *Chem. Mater.*, 2012, **24**, 3231–3239.
22 T. Nishitoba, N. Yoshida, J. N. Kondo and T. Yokoi, *Ind. Eng. Chem. Res.*, 2018, **57**, 3914–3922.
23 T. Nishitoba, T. Nozaki, S. Park, Y. Wang, J. N. Kondo, H. Gies and T. Yokoi, *Catalysts*, 2020, **10**, 1204.
24 K. Yamamoto, S. E. B. Garcia, F. Saito and A. Muramatsu, *Chem. Lett.*, 2006, **35**, 570–571.
25 S. E. B. Garcia, K. Yamamoto and A. Muramatsu, *J. Mater. Sci.*, 2008, **43**, 2367–2371.
26 M. Yabushita, M. Yoshida, F. Muto, M. Horie, Y. Kunitake, T. Nishitoba, S. Maki, K. Kanie, T. Yokoi and A. Muramatsu, *Mol. Catal.*, 2019, **478**, 110579.
27 K. Kanie, M. Sakaguchi, F. Muto, M. Horie, M. Nakaya, T. Yokoi and A. Muramatsu, *Sci. Technol. Adv. Mater.*, 2018, **19**, 545–553.
28 M. Yabushita, H. Kobayashi, R. Osuga, M. Nakaya, M. Matsubara, S. Maki, K. Kanie and A. Muramatsu, *Ind. Eng. Chem. Res.*, 2021, **60**, 2079–2088.
29 T. Xiao, M. Yabushita, T. Nishitoba, R. Osuga, M. Yoshida, M. Matsubara, S. Maki, K. Kanie, T. Yokoi, W. Cao and A. Muramatsu, *ACS Omega*, 2021, **6**, 5176–5182.
30 M. Kakihana and M. Yoshimura, *Bull. Chem. Soc. Jpn.*, 1999, **72**, 1427–1443.
31 K. Yoshizawa, H. Kato and M. Kakihana, *J. Mater. Chem.*, 2012, 22, 17272–17277.
32 M. Haouas, F. Taulelle and C. Martineau, *Prog. Nucl. Magn. Reson. Spectrosc.*, 2016, **94–95**, 11–36.
33 M. Yabushita, M. Yoshida, R. Osuga, F. Muto, S. Iguchi, S. Yasuda, A. Neya, M. Horie, S. Maki, K. Kanie, I. Yamanaka, T. Yokoi and A. Muramatsu, *Ind. Eng. Chem. Res.*, 2021, 60, 10101–10111.
34 D. E. Akporiaye, I. M. Dahl, H. B. Mostad and R. Wendelbo, *J. Phys. Chem.*, 1996, **100**, 4148–4153.
35 Y. A. Ivanov, N. Lewyckyj, S. E. Levchuk, B. S. Prister, S. K. Firsakova, N. P. Arkhipov, A. N. Arkhipov, S. V. Kruglov, R. M. Alexakhin, J. Sandalls and S. Askbrant, *J. Environ. Radioact.*, 1997, **35**, 1–21.
36 G. Steinhauser, A. Brandl and T. E. Johnson, *Sci. Total Environ.*, 2014, **470–471**, 800–817.
37 M. Castrillejo, N. Casacuberta, C. F. Breier, S. M. Pike, P. Masqué and K. O. Buesseler, *Environ. Sci. Technol.*, 2016, **50**, 173–180.

